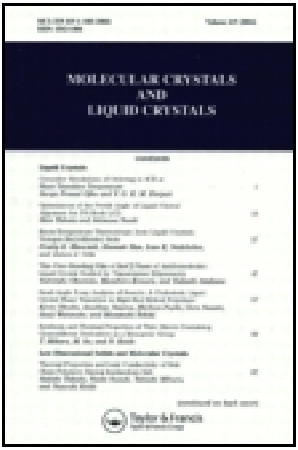

Molecular Crystals and Liquid Crystals

VIBRATIONAL SPECTROSCOPIC INVESTIGATIONS OF 4-ALKYL 4′-CYANO BIPHENYLS [C_nH_{2n+1}-C_6H_5-C_6H_5-CN, n = 9, 10 and 11]

K. V. G. K. Murty [a] , T. Manisekharan [a] & T. K. K. Srinivasan [a]

[a] Regional Sophisticated Instrumentation Centre, Department of Chemistry, Indian Institute of Technology Madras, Chennai-600 036, India

Version of record first published: 15 Jul 2010

To cite this article: K. V. G. K. Murty, T. Manisekharan & T. K. K. Srinivasan (2004): VIBRATIONAL SPECTROSCOPIC INVESTIGATIONS OF 4-ALKYL 4′-CYANO BIPHENYLS [C_nH_{2n+1}-C_6H_5-C_6H_5-CN, n = 9, 10 and 11], Molecular Crystals and Liquid Crystals, 408:1, 83-102

To link to this article: http://dx.doi.org/10.1080/15421400490428259

Mol. Cryst. Liq. Cryst., Vol. 408, pp. 83–102, 2004
Copyright © Taylor & Francis Inc.
ISSN: 1542-1406 print/1563-5287 online
DOI: 10.1080/15421400490428259

Taylor & Francis
Taylor & Francis Group

VIBRATIONAL SPECTROSCOPIC INVESTIGATIONS OF 4-ALKYL 4′-CYANO BIPHENYLS [C_nH_{2n+1}-C_6H_5-C_6H_5-CN, n = 9, 10 AND 11]

*K. V. G. K. Murty, T. Manisekharan, and T. K. K. Srinivasan**
Regional Sophisticated Instrumentation Centre,
Department of Chemistry, Indian Institute of Technology
Madras, Chennai–600 036, India

A complete vibrational analysis of liquid crystals 4-alkyl 4′-cyano biphenyls [C_nH_{2n+1}-C_6H_5-C_6H_5-CN, n = 9, 10 and 11] is presented. The vibrational assignments are discussed in relation to their respective crystal structures. The vibrational bands in the CH stretching as well as CH_2 wagging regions are effectively correlated to the crystal structures of the respective compounds. The ratios of IR and Raman intensities of the bands in the CH stretching region reveal the presence of disorder in the compounds.

Keywords: FT-IR; Liquid Crystals; Raman

INTRODUCTION

The intimate correlation of the alkane chains with the arrangement of complex molecules in biological and polymer assemblies has led to the use of infrared and Raman spectra as diagnostic of chain conformation and the structure of molecular assembly [1,2]. The study of amorphous phases has held considerable challenge and interest, particularly in liquid crystals, when dealing with the local dynamic structures [3,4] and the orientational behavior [5–7]. There exists one or more phases between the crystalline state and isotropic liquid phase in liquid crystals. The molecular shape and the polar–polar interactions allow the molecules to align in partially ordered arrays. These structures include lamellar, cubic, two dimensional, rectangular, tetragonal, and hexagonal packings [8–12]. With increasing temperature, the liquid crystals show a transition from a highly ordered crystalline phase to liquid crystalline phases like smectic, nematic, and

---

K. V. G. K. Murty gratefully acknowledges the financial support by IIT Madras, Chennai.
*Corresponding author. tkksrinivasan@hotmail.com

other phases, where molecules are oriented in various ways along the plane and disorder can be present between the planes.

Alkyl and alkoxy cyano biphenyls are popular liquid crystals that are suitable for use in electro-optic devices, and their properties as liquid crystal devices have been well established [11,12]. The room temperature crystal structures of 4-nonyl 4′-cyano biphenyl, 4-decyl 4′-cyano biphenyl, and 4-undecyl 4′-cyano biphenyl (abbreviated as C_9, C_{10}, and C_{11}, respectively) are reported from this laboratory [13–15]. The crystal structure reveals the packing differences in these compounds, where the biphenyl moiety is attached to an alkyl side chain with a sequence of 8, 9, and 10 methylene groups. The CH_2 group absorption in compounds containing polymethylene chains have been found to depend on the nature of chain packing (subcell) [16]. Inter- and intrachain interactions of the alkyl chain dictate different ways of molecular packing. In orthorhombic and monoclinic subcell packing, symmetry considerations and interchain distances favor interaction leading to splitting of certain CH_2 fundamental modes. In the hexagonal subcell, on the other hand, both symmetry considerations and interchain distances, which are practically the same as in the liquid, rule out the possibility of such splitting. In the triclinic subcell, there is only a single chain in the unit cell and there is only a single component for every fundamental. 4-pentyl 4′-cyano biphenyl and 4-dodecyl 4′-cyano biphenyl appear to be the only compounds for which possible assignments of the Raman spectra have been reported [9,10]. Many of the earlier phase transition studies were devoted to CN and phenyl ring vibrations [5–9]. The present investigation reports a detailed vibrational analysis of the alkyl vibrations for C_9, C_{10}, and C_{11} compounds, respectively, in relation to their crystal structure, in addition to the analysis of the phenyl ring and CN stretching vibrations.

EXPERIMENTAL METHODS

Commercially available alkyl cyano biphenyls are obtained from British Drug Houses (BDH) Ltd. (Poole, U.K.), and used without further purification. The FT-Raman spectra are recorded using a Bruker IFS66v Fourier transform infrared (FTIR) spectrometer with FRA-106 Raman module attached. A Nd-YAG laser operating at 1064 nm wavelength with 100 mW power and 2 μm beam diameter is used as the Raman excitation source. The scattered radiation is collected through 180° back scattering geometry. The spectra are recorded with 2 cm^{-1} resolution. The infrared spectra are recorded using a Bruker IFS 66 v FTIR spectrometer in the range 4000–400 cm^{-1} with 2 cm^{-1} resolution. All the spectra are averaged over 200 scans. The FTIR spectra are recorded using pellets made of KBr and sample in a 20:1 ratio. The KBr pellets are preheated with an IR lamp to eliminate any possible contamination of moisture.

CRYSTAL STRUCTURE ANALYSIS

In order to consider the vibrational spectrum of the crystalline state and to understand the molecular vibrations, a brief description of the crystal structure of the compounds is presented [13–15]. The alkyl cyanobiphenyls (C_9, C_{10}, and C_{11}) crystallize into two different space groups. The C_9 and C_{11} homologues crystallize in the triclinic space group P_1, whereas C_{10} crystallizes in monoclinic space group $P2_{1/n}$ [13–15]. The unit cell parameters of these compounds are given in the Table I.

The C_9 exists as pair of molecules in the unit cell of the crystal as shown in Figure 1(a) [13]. The dihedral angle between the phenyl rings of molecule I is 35.97° and in molecule II is 29.83°. This indicates that the two molecules in the asymmetric unit cell will have different conformations. Overlapping of the biphenyl portion is observed in the packing, and the pair of molecules form an antiparallel arrangement (see Figure 2(a)) [13]. The torsion angle between the alkyl chain and the phenyl ring also differ from molecule I to molecule II significantly. The torsion angle for molecule I is 178.89°, whereas for molecule II the angle is 159.98°. The terminal C≡N dipoles interact with the phenyl rings of the neighboring molecule, as shown in Figure 2(a) [13].

In contrast to C_9, the C_{10} has different crystal structure and packing (see Figure 1b) [14]. The molecules exist as single entities in the unit cell. The phenyl rings of the biphenyl moiety are nearly coplanar with a dihedral angle of 2.2°. The torsion angle between the linear alkyl chain and the phenyl ring of the biphenyl is 73.91°. The packing diagram shows that the

TABLE I Unit Cell Parameters of C9, C10, and C11

	C_9	C_{10}	C_{11}
a, Å	9.765	15.813	9.755
b, Å	11.460	5.479	11.32
c, Å	17.86	23.179	19.91
α, °	85.46	90	96.86
β, °	80.87	90	94.41
γ, °	71.63	102.2	109.16
V, Å^3	1871.9	1963	2046.46
Z	4	4	4

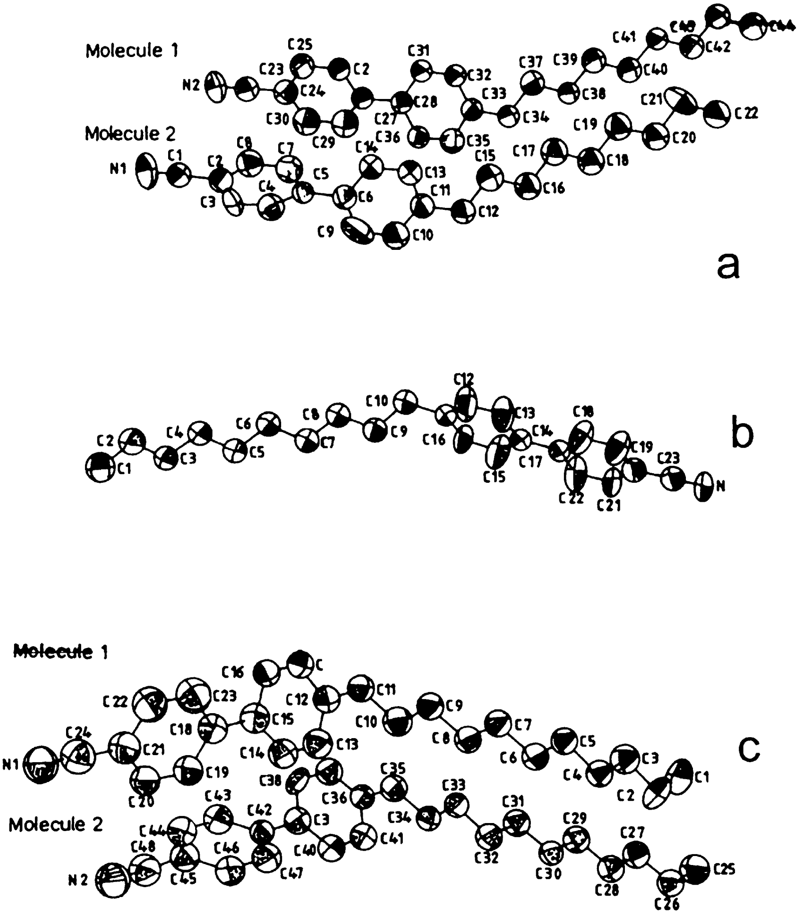

FIGURE 1 ORTEP Diagrams of (a) C_{11}, (b) C_{10}, and (c) C_9.

molecules in one sheet form a head-to-tail antiparallel configuration (see Figure 2(b)) [14].

The crystal structure of the C_{11} is very similar to that of C_9 (Figure 1(c)) [15]. The dihedral angle between the phenyl rings in molecule I is 30.19° and in molecule II is 35.83°, and the two molecules in the asymmetric unit cell have different conformations [15]. In the asymmetric unit cell, the pair of molecules forms an antiparallel arrangement, with their N≡C dipoles attracting each other (see Figure 2(c)) [15]. The overlapping of the biphenyl portion is also observed. The cohesion between the molecules is predominant through the dipolar interactions (see Figure 2(c)) [15].

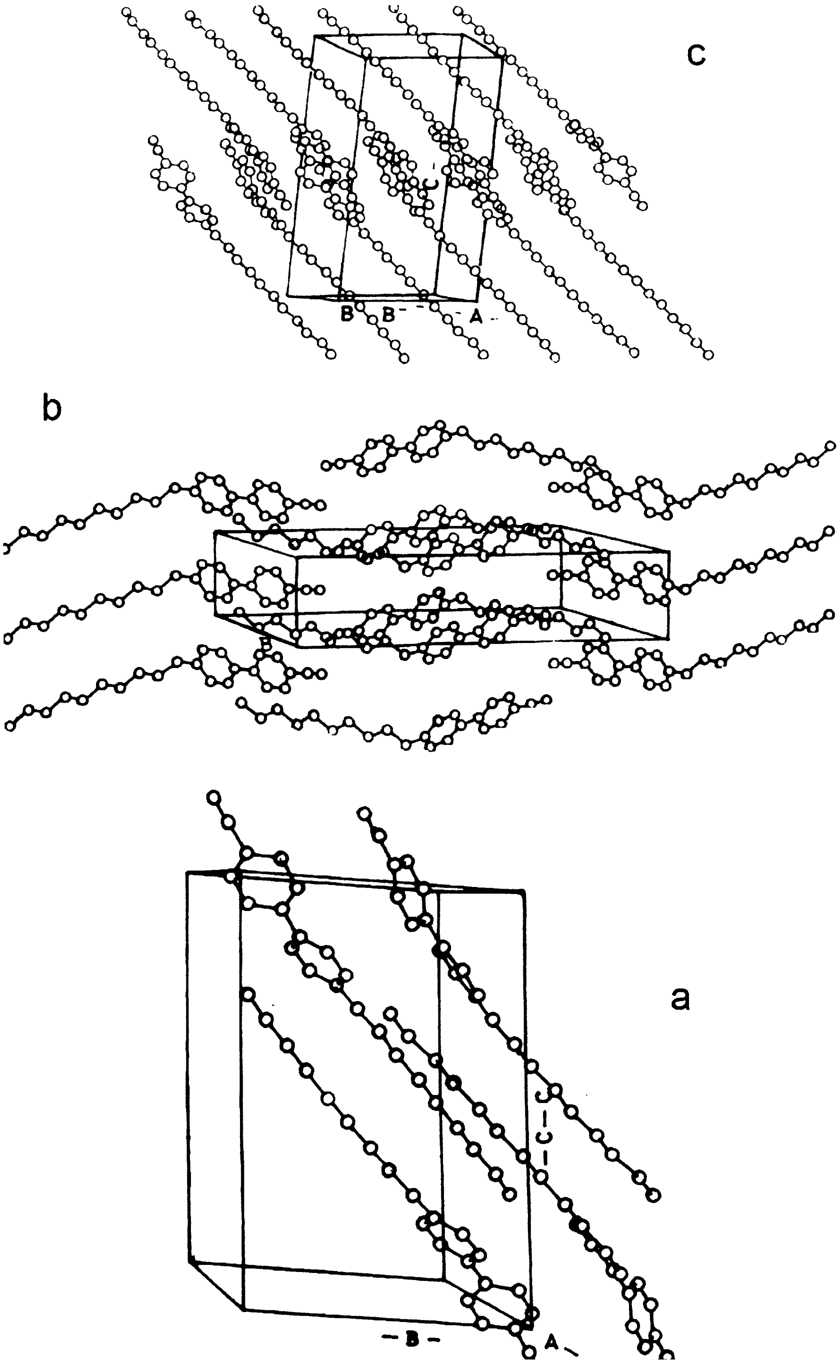

FIGURE 2 ORTEP Diagrams of (a) C_{11}, (b) C_{10}, and (c) C_9.

The above crystal structure information shows the structural similarities between C_9 and C_{11} and also their differences in relation to the structure of C_{10}. These compounds differ only in the number of CH_2 groups. The number of CH_2 groups present is ***even*** in C_9 and C_{11} and ***odd*** in C_{10}. This factor gives rise to the differences in the conformation of the alkyl chains and thereby the molecular arrangement.

RESULTS AND DISCUSSION

The vibrational spectra of alkyl cyano biphenyls consist of vibrations characteristic of alkyl chains, biphenyl moiety, and CN stretching mode. The CN stretching mode exists as an isolated mode, away from congested region of the alkyl and biphenyl modes. The alkyl chain vibrations include the CH stretching modes of CH_2 and CH_3 groups, CH_2 and CH_3 deformations, and CC skeletal vibrations and CCC bending vibrations. A detailed description and analysis of the above vibrations of the three compounds considered is given below.

Alkyl Chain Modes

The vibrational frequencies of hydrocarbon chains in *n*-alkanes form the basis of interpretation of the alkyl chains present in the alkyl-cyano-biphenyls [16–26]. Detailed analysis of *n*-alkane spectra are available in the literature [20–26], so that the origin of the vibrational frequencies of the all-trans chain conformation present in these systems can be understood well. For an alkyl chain with n atoms per repeat unit and M repeat units, there are 3nM modes of vibration that occur in 3n frequency branches. Within each branch, the frequency of each of the M possible modes depends upon the relative phase of the nuclear displacements of the neighboring units, each mode being characterized by a phase angle ϕ_k, where $\phi_k = k\pi/M$, with $k = 0, 1, 2 \cdots M\text{-}1$. For an infinite polymer such as polyethylene, only those modes with $k = 0$ are allowed both in the IR and Raman spectra (i.e., the vibrations in each repeat unit are totally in phase). For segments of chains that are less than infinite in length, or disordered due to "gauche" rotamer formation, the above selection rules are not vigorous, and vibrations corresponding to other k values will become active. The frequency of certain vibrations with $k = 0$ will be a function of the all-trans segment length present in the CH_2 oligomer, thus providing useful structural probes in systems with long alkyl chains. In a highly ordered chain of infinite length, the CH_2 modes exist for all values of ϕ (phase angle). For these modes to be vibrationally active the value of ϕ must be 0 or π. The vibrational modes are Raman active when the phase angle is 0 and IR active when the phase angle is π. Thus the fundamentals $d^{\pm}(0)$ and $\delta^{\pm}(0)$ are Raman active and $d^{\pm}(\pi)$ and $\delta^{\pm}(\pi)$ are IR active [24].

The alkyl chain vibrational modes are denoted by Snyder et al. [24] in the following manner: d^+ and d^- are the symmetric and antisymmetric CH stretching modes of methylene group, r^+ and r^- are the symmetric and antisymmetric (degenerate) CH stretching modes of methyl group, δ is the HCH deformation, and P denotes the methyl rocking vibration. The internal vibrations of the alkyl chains in alkyl cyano biphenyls are assigned in comparison with the spectra of *n*-alkane fatty acid esters and other systems containing long alkyl chains in addition to the spectra of *n*-alkanes, [16, 20–26]. The frequencies and the assignments of the observed vibrations in IR and Raman spectra are listed in Tables II and III.

CH Stretching Region

The C–H stretching region of C_9, C_{10}, and C_{11} consists of C–H symmetric and asymmetric stretching vibrations of methyl and methylene groups. The CH stretching vibrations due to the aromatic moiety are also part of this region. The carbon hydrogen stretching vibrations that occur in IR and Raman spectra in the region 2800–3100 cm^{-1} are shown, respectively, in Figures 3(a) and 3(b). Assignments of the CH stretching modes of methyl and methylene groups are given in Table II.

In general, vibrations due to the symmetric (d^+) and asymmetric (d^-) CH stretching modes of methylene groups in IR spectra (Figures 3(a)) appear at 2850 cm^{-1} and 2920 cm^{-1}, respectively, and in Raman spectra

TABLE II Vibrational Assignments CH Stretching Modes of Alkyl Chains

Frequency of IR active modes (cm^{-1})					Frequency of Raman active modes (cm^{-1})				
Mode	C_9	C_{10}	C_{11}	Assignment	Mode	C_9	C_{10}	C_{11}	Assignment
$d^-(\pi)$	2920	2917	2920	Asymmetric CH stretch of (CH_2)	$d^-(0)$	2880	2880	2879	Asymmetric CH stretch (CH_2)
r^+	2866	2864	2866	Symmetric CH stretch (CH_3)	r^+	2868	2868	2866	Symmetric CH stretch (CH_3)
$d^+(\pi)$	2849	2845	2847	Symmetric CH stretch (CH_2)	$d^+(0)$	2847	2849	2847	Symmetric CH stretch (CH_2)
r^-	2964	2964	2963	Symmetric CH stretch (CH_3)	r^-	2963	2962	2961	Symmetric CH stretch (CH_3)

TABLE III Vibrational Assignments for C_9, C_{10}, and C_{11}

C_9		C_{10}		C_{11}		
IR	Raman	IR	Raman	IR	Raman	Assignment
411	429	405	—	412	405	Ring-out-of-plane deformation
474	471	470	466	474	437	
527	523	514	515	526	522	
551	551	546	545	550	564	
637	635	636	635	636	635	
650	651	660	660	650	650	
720	729	720	736	720	729	CH_2 rocking
—	744	—	754	—	736	
776	—	780	779	776	769	C–H out-of-plane deformation
807	804	810	813	807	802	
824	824	834	834	822	824	
—	854	—	856	—	852	
885	885	889	890	884	883	CH_3 rocking
1003	1004	1012	1004		1004	Interring C–C stretching
1019	1024	—	1022	1018	1024	C–C stretching
—	1049	—	—	—	—	
1061	1065	1070		1060	1075	
—	—	—	1088	1074	—	
—	1113	—	—	—	1114	In-plane ring HCC bending
1121	1126	1124	—	—	—	
1179	1179	1186	1180	1179	1180	
1244	—	1221	—	—	1237	Ring-CH_2 C–C stretching
1287	1285	1282	1280	1287	1284	
—	—	—	—	—	1298	
1314	1311	—	1313	1313	1313	
1326	1324	1332	1326	—	1327	CH_2 wagging
—	—	—	1338	—	—	
1348	1348	1349	1351	—	1348	
—	—	—	—	—	1358	
1374	1370	1368	1373	1372	1373	CH_3 umbrella deformation
—	1396	—	1400	—	1396	CH_2 scissoring
—	1419	—	1423	—	1422	
1442	1437	1438	—	1441.5	1439	
1456	1466	—	1467	1460	1467	
—	1493	—	1492	—	1493	Ring C=C stretching
1522	1519	1524	1517	1520	1518	
1605	1604	1604	1604	1605	1604	
2220	2220	2226	2226	2220	2220	CN stretching
3032	—	—	3023	—	3030	Aromatic CH stretching
3070	3070	3073	3070	3070	3070	

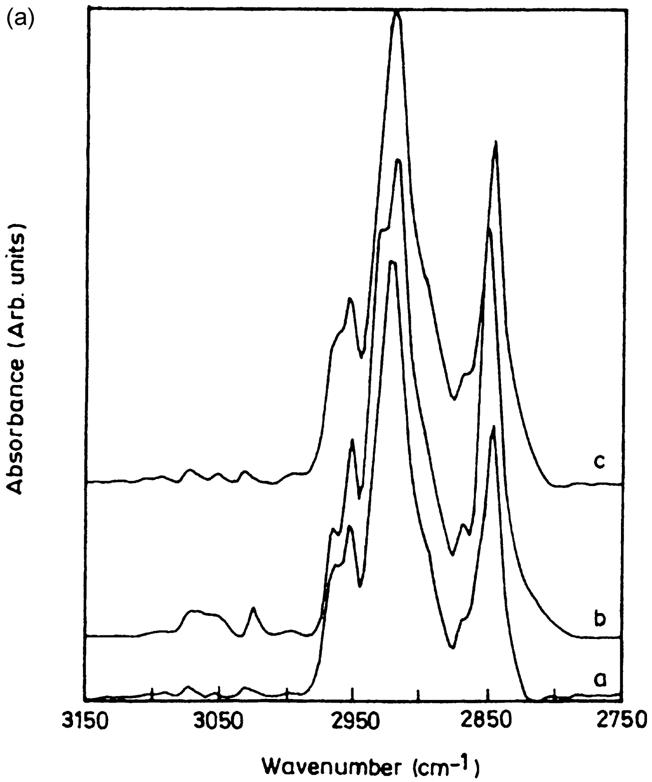

FIGURE 3(a) CH stretching region (3150–2750 cm^{-1}) FT-IR spectra of a, C_9; b, C_{10}; and c, C_{11}. (3b) CH stretching region (3150–2750 cm^{-1}) FT-Raman spectra of a, C_9; b, C_{10}; and c, C_{11}.

(Figures 3(b)) the same bands appear at 2850 cm^{-1} and 2880 cm^{-1}. The symmetric CH stretching mode (r^+) of the methyl group is observed at 2870 cm^{-1}, whereas the in-plane (r_a^-) and out of plane (r_b^-) asymmetric stretching modes of the methyl group appear around 2960 cm^{-1} and 2950 cm^{-1}, respectively, in both the IR and Raman spectra (see Figures 3(a) and 3(b)) [26]. In addition to these bands, overtones and combinations of methyl and methylene deformations also appear in this region. This spectral region is further complicated by the presence of the Fermi resonance components of the CH_2 stretching vibrations with the overtones and combinations of the CH_2 scissoring modes, occurring around 1460 cm^{-1} [20–26].

In the IR spectrum, in addition to the above bands, a shoulder appears at 2893 cm^{-1} (Figure 3(a)), which is an overtone or combination band of the CH_2 deformation modes. Another shoulder at 2930 cm^{-1} in the IR spectrum

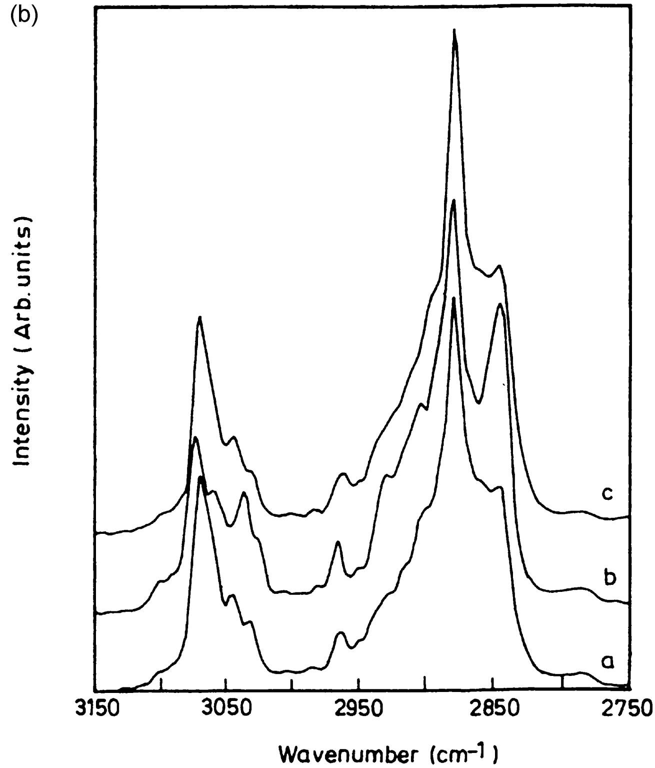

FIGURE 3(b) Continued.

of C_{10}, as shown in Figure 3(a), is a Fermi resonance component of d^+ and the above-mentioned overtone or combination band [26]. The FT-Raman spectra (see Figure 3(b)) of alkyl cyano biphenyls contains a strong peak at 2880 cm^{-1} assigned to asymmetric (d^-) CH stretching vibration, and its Fermi resonance component appears as a shoulder at 2934 cm^{-1}. The well resolved feature at 2845 cm^{-1} in the spectrum of C_{10} is the symmetric CH stretching vibration (d^+), and the same mode appears as a broad shoulder in C_9 and C_{11} compounds. The shoulder observed in the spectra of these compounds around 2905 cm^{-1} is a background band, which, according to Snyder et al. present as a consequence of d^+ undergoing Fermi resonance [22].

In the IR spectrum, it is interesting to see from Figure 3(a) that the methylene asymmetric stretch d^- at 2920 cm^{-1} is equally intense in all the three compounds, whereas the intensity of asymmetric stretch d^+ at 2850 cm^{-1} is higher in C_{10} relative to that observed for C_9 and C_{11}. The same vibration d^+, which appears as a shoulder in Raman spectra (see Figure

3(b)), is also more intense in C_{10} compared to C_9 and C_{11}. Similarly, the most intense band at 2880 cm^{-1} assigned to methylene asymmetric stretch (d^-) is of equal in intensity in the Raman spectra of C_9, C_{10}, and C_{11}.

In general, the CH stretching vibrations are considered to be highly localized and relatively insensitive to the molecular conformation and interchain packing in comparison with the methylene bending and rocking vibrations. Snyder and coworkers [24–26] established strong correlation between the relative intensities of the bands in this region with inter-and intramolecular order of the polymethylene chains. This correlation is due to the Fermi resonance interaction between the CH stretching vibrations and the overtones/combinations of CH_2 scissoring vibrations of alkyl chains. The methylene scissoring vibrations involved in the resonance are sensitive to both chain conformation and lateral interchain interactions. It is also well known that the CH_2 deformations undergo significant intermolecular coupling. It is possible to distinguish two levels of Fermi resonance interaction depending on the dispersion of the CH_2 deformations with respect to the chain axis. The first one involves the dispersion of CH_2 deformation modes parallel to the chain axis. This is normally the case in isolated alkyl chains. The second is due to intermolecular interaction resulting in the dispersion of CH_2 deformation modes perpendicular to the chain axis. Thus the disorder present in both the isolated chains and lateral chain interaction can be investigated. The peak intensity ratios of the CH stretching bands are used for the study of the disorder in systems containing alkyl chains. Although the Fermi resonance may affect the distribution of intensity in dramatic ways, it is not expected to alter the integrated intensity of the fundamentals.

In *n*-alkanes, the Raman intensity ratio I_{2880}/I_{2850} was taken as a measure of lateral chain disorder [23] and with the increase in disorder it was noted that the above-mentioned ratio decreases. It must be noted here that the use of the above ratio as a measure of disorder is appropriate only in the absence of significant conformational disorder [24]. The IR intensity ratios of 2920 and 2850 cm^{-1} bands (i.e., I_{2920}/I_{2850}) of C_9, C_{10}, and C_{11} are 1.59, 1.17, and 1.36, respectively. The Raman intensity (I_{2880}/I_{2850}) ratios of C_9, C_{10}, and C_{11} are 1.97, 1.38, and 1.88, respectively. From this it can be readily concluded that, the ordering of C_{10} is different from C_9 and C_{11}, and also that the C_{10} system is more disordered than C_9 and C_{11} [23].

In the IR spectrum, the aromatic CH stretching modes are more intense in the C_{10} compound compared to that for C_9 and C_{11}, where the intensities of the bands in the range 3000 cm^{-1} to 3100 cm^{-1} are extremely low. The same modes are found to be of equal intensity in the Raman spectra of C_9, C_{10}, and C_{11}. As expected, these bands are of greater intensity in the Raman spectra when compared with the IR because of the strong polarizability of the phenyl rings [27–30].

CH_2 Scissoring and Wagging Vibrations

The other important vibrations of methylene groups are the deformations, which are classified as scissoring, wagging, twisting, and rocking modes in order of decreasing frequency. Splitting of certain fundamentals may occur due to the interaction between adjacent methylene groups within polymethylene chains in certain subcell packings [16]. The band progression in both IR and Raman (see Figures 4 and 5), extending from 1420 cm^{-1} to 1490 cm^{-1}, is assigned to the CH_2 scissoring vibrations. The prominent peaks in this progression are centered around 1466 cm^{-1}, 1455 cm^{-1}, 1438 cm^{-1}, and 1420 cm^{-1}. These peaks are more intense in C_9 and C_{11} than in the C_{10} counterpart. The other important branch of methylene deformation bands is the wagging modes that occur around 1350 cm^{-1}. Like the scissoring modes, the wagging modes also are more intense in C_9 and C_{11} compared to those of C_{10} (Figures 4 and 5). In general, the scissoring and wagging modes are more intense in the spectra of C_9 and C_{11} than in C_{10}. The 1370 cm^{-1} component of the spectra is due to the CH_3 deformation that is insensitive to the conformational changes. The peak position of this band is normally used as an internal standard to analyze the disorder present in the system [33,34]. Four bands in this region, 1365, 1355, 1340, and 1305 cm^{-1}, indicate the presence of gauche-related con-

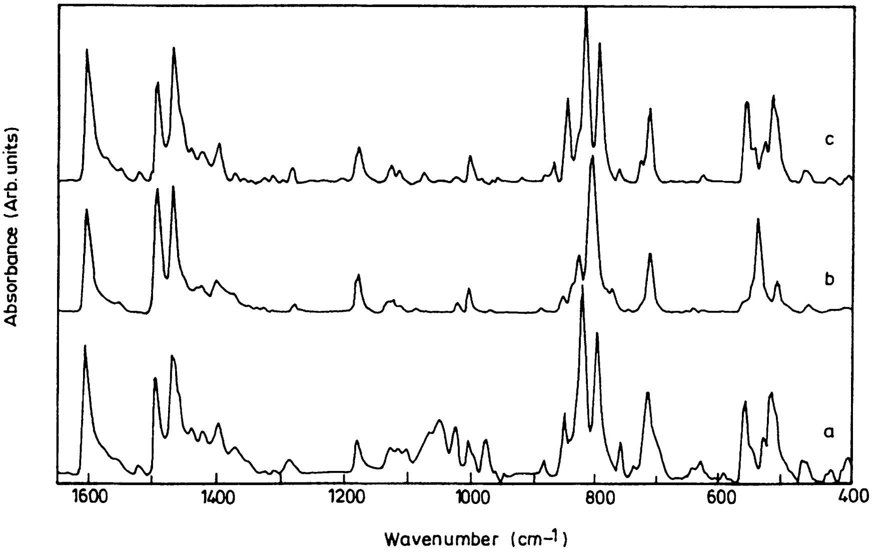

FIGURE 4 FTIR spectra of a, C_9; b, C_{10}; and c, C_{11} in the range 1650–400 cm^{-1} (note the similarities in the spectra of C_9 and C_{11}).

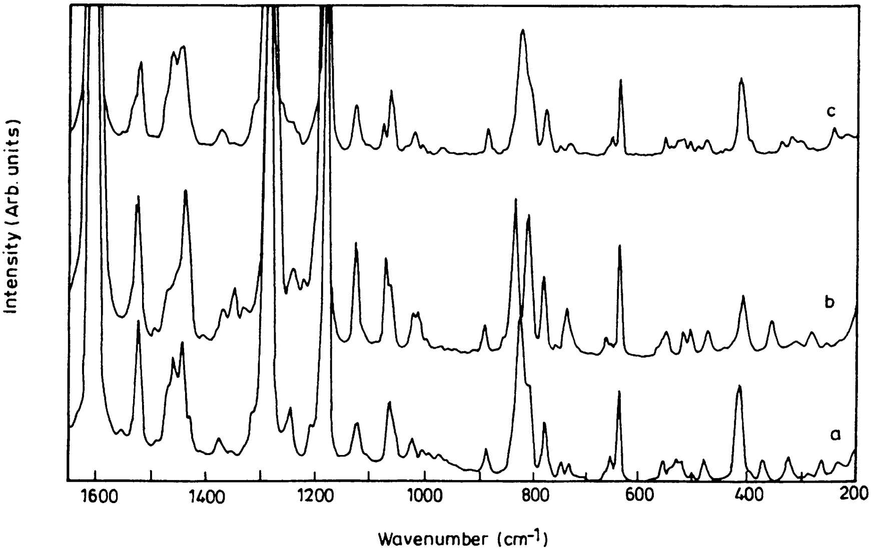

FIGURE 5 FT-Raman spectra of a, C_9; b, C_{10}; and c, C_{11} in the range 1650–200 cm^{-1}.

formers. These bands, which are shown to be due to localized CH_2 wagging vibrations, are extremely sensitive to the changes in the conformation of the chain, especially to the formation of gauche rotamers in alkyl chains [33,34]. The intensity differences observed in the bands occurring in the wagging region of the three compounds indicate the differences in the orientation of these systems.

CH_2 and CH_3 Rocking Modes

The methylene rocking band appears at 729 cm^{-1} in the Raman spectra of C_9 and C_{11} as shown Figure 5, and the same band is observed at 736 cm^{-1} in C_{10}. The intensity of this band is higher in the spectrum of C_{10} than in C_9 and C_{11} spectra. In the FTIR spectra (see Figure 4), the above vibration occurs at 720 cm^{-1} in all these compounds. This band has a shoulder around 730 cm^{-1} (see Figure 4). In polymethylene chains, the splitting of the band at 720 cm^{-1} to 720 and 730 cm^{-1} has been attributed to intermolecular interaction by Snyder et al. [26], revealing order and disorder imperfections [20–26]. The differences of the CH_2 rocking mode frequencies and intensities reveal the differences in crystal packing in C_9, C_{10}, and C_{11}.

The terminal methyl group gives rise to bands at 1470 cm^{-1}, 1370 cm^{-1}, and 890 cm^{-1} in the IR spectrum which are due to methyl out-of-plane deformation, in plane deformation, and rocking vibrations, respectively. The CH_3 rocking vibration appears at 885 cm^{-1} in both the IR and Raman spectra of C_9 and C_{11}. The same vibration has a peak at 890 cm^{-1} in Raman and IR spectra of C_{10}. This frequency shift of the CH_3 rocking mode can be attributed to the differences in the end chain conformation between C_9 and C_{11} with that of C_{10}. By and large, these CH_3 deformations, both in plane and out of plane, are quite insensitive to the conformational changes taking place in the system and have been used as an internal standard while analyzing the disorder of the system [16–19,21,22].

C–C Stretching Region

The region between 1000–1150 cm^{-1} consists of C–C stretching vibrations of the alkyl chains present in C_9, C_{10}, and C_{11}. In the IR spectrum the bands occurring in this region of the C_9 compound are much more intense compared with the intensity of C_{10} and C_{11} (see Figure 4). The bands in the Raman spectra (see Figures 5 and 6) occurring at 1060 cm^{-1} and 1190 cm^{-1} are associated with the trans conformation, and the band at

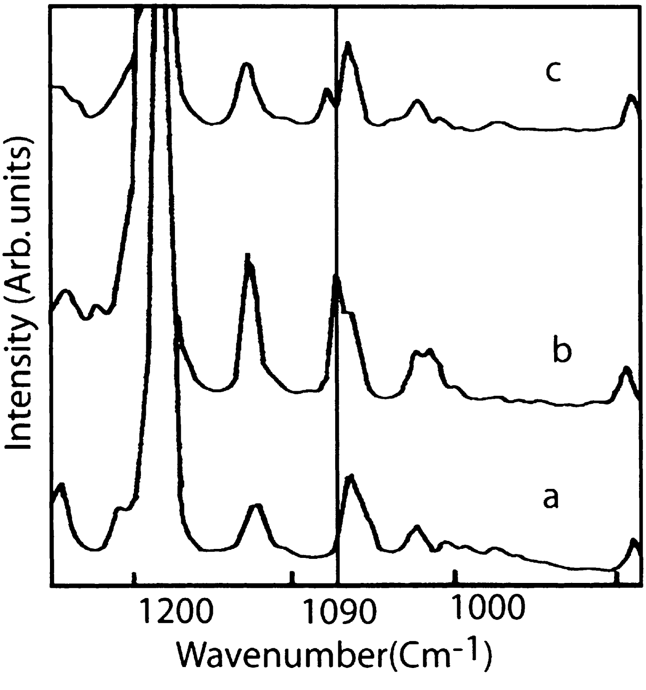

FIGURE 6 CC stretching region in FT-Raman spectra of a, C_9; b, C_{10}; and c, C_{11}. Note the intensity differences in 1090 cm^{-1} peak attributed to gauche rotomers.

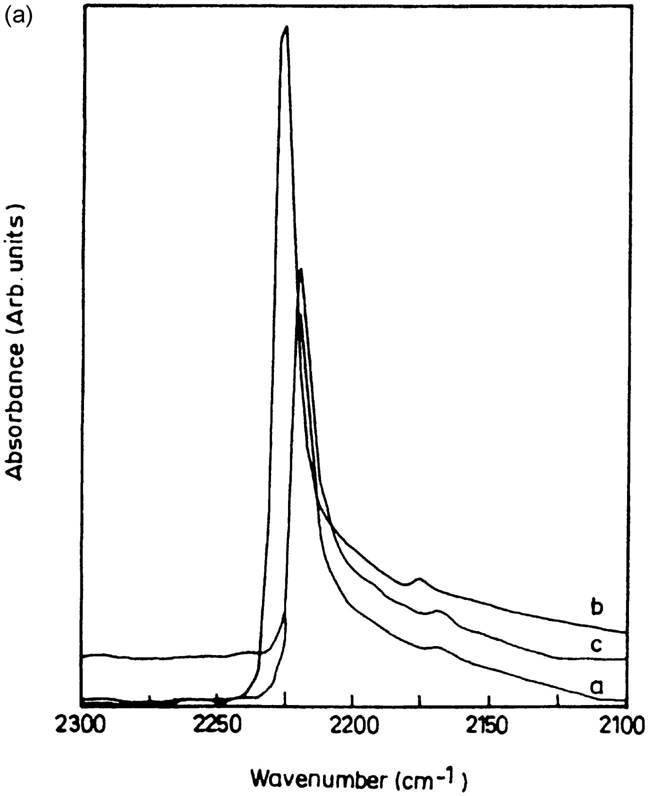

FIGURE 7(a) FTIR spectra of CN stretching region (2300–2100 cm^{-1}) of a, C_9; b, C_{10}; and c, C_{11}. Note the frequency shift in C_{10}. (7b) FT-Raman spectra of CN stretching region (2300–2100 cm^{-1}) of a, C_9; b, C_{10}; and c, C_{11}. Note the frequency shift in C_{10}.

1090 cm^{-1} is assigned to gauche conformation. All the three compounds show bands with similar intensity at 1060 cm^{-1} and 1190 cm^{-1} shows the presence of trans rotomers. The presence of the band of moderate intensity at 1090 cm^{-1} in C_{10} indicates the presence of gauche rotomers at room temperature. The same band occurs with low intensity in C_{11} and probably part of the 1060 cm^{-1} band in C_9. The above observation is consistent with the observation of CH stretching region, where from the intensity ratios it is inferred that the disorder present in the C_{10} is more than that of C_9 and C_{11}.

As shown in Figures 4 and 5, the bands appearing around 1004 cm^{-1} and 1285 cm^{-1} are attributed to the C–C stretch of the biphenyl link and C–C stretch of CH_2 group adjacent to the phenyl ring respectively [27–32]. In the IR spectra the 1285 cm^{-1} band shifts to the lower side in the case of C_{10}

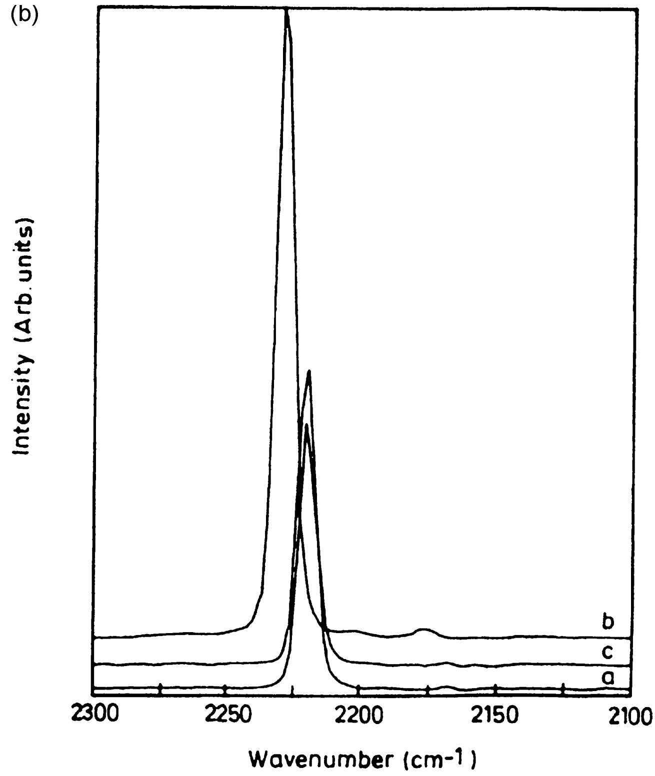

FIGURE 7(b) Continued.

with respect to the peak positions of C_9 and C_{11}, whereas in Raman the peak positions are same in all the compounds.

C–N Stretching Vibration

The C–N stretching vibration in C_9 and C_{11} appears at $2220\,cm^{-1}$, and the same vibration in C_{10} occurs at $2226\,cm^{-1}$ in both IR and Raman spectra (see Figures 7(a) and 7(b)). The IR and Raman intensities of C≡N stretching modes of C_9 and C_{11} are almost same. The IR intensity of this band in C_{10} is lower than that of C_9 and C_{11}, whereas in Raman the same vibration of C_{10} is twice as intense as those of C_9 and C_{11} (see Figures 7(a) and 7(b)). The coplanarity of the two-phenyl rings induces strong polarizability of the biphenyl moiety, which results in higher Raman intensity. The greater orbital overlap (see Figure 2) of C≡N group with the phenyl rings of the neighboring molecules as they lie almost in the same plane, giving rise to higher π interaction across the biphenyl moiety, is reflected in the higher position (2226 cm^{-1}) of CN stretching vibration in C_{10} [14].

Phenyl Ring Vibrations

The biphenyl moiety of the alkyl cyano biphenyls is interpreted in comparison with the vibrational spectra of biphenyls and cyano biphenyls [27–32]. Vibrations due to the biphenyl moiety occur at 1520 cm^{-1}, and 1605 cm^{-1}, as shown in Figures 4 and 5. These are due to the ring stretching or C–C stretching vibrations of the phenyl ring. In both the IR and Raman spectra, as shown in Figures 8(a) and 8(b), the peak position of the vibration occurring at 1605 cm^{-1} remains the same in all the compounds, but the intensities show considerable changes. In the IR spectra, the intensities of C_9 and C_{11} bands are equal, whereas that of C_{10} band is

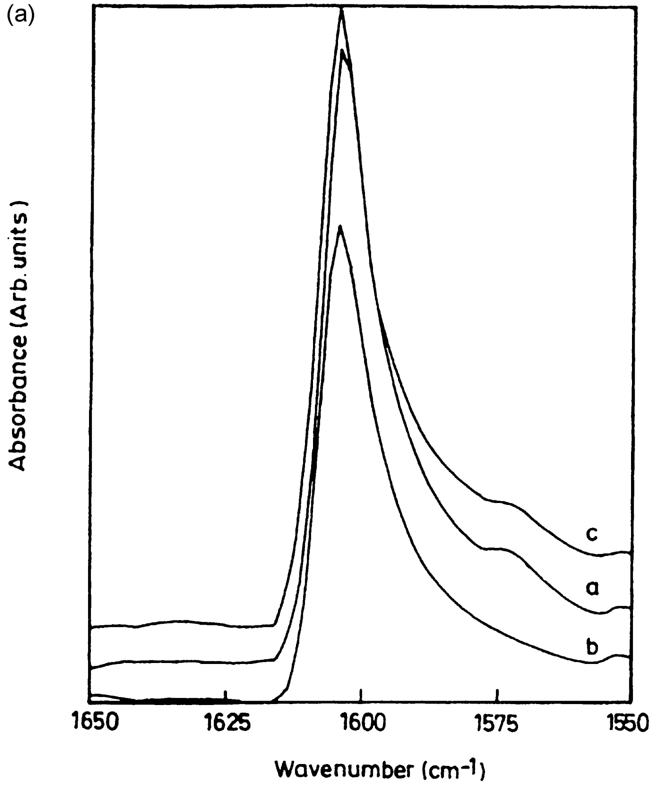

FIGURE 8(a) FTIR spectra of a, C_9; b, C_{10}; and c, C_{11}. Note the differences in frequency and intensity of aromatic CC stretching mode at 1605 cm^{-1}. (8b) FT-Raman spectra of a, C_9; b, C_{10}; and c, C_{11} in the range 1650–1550 cm^{-1}.

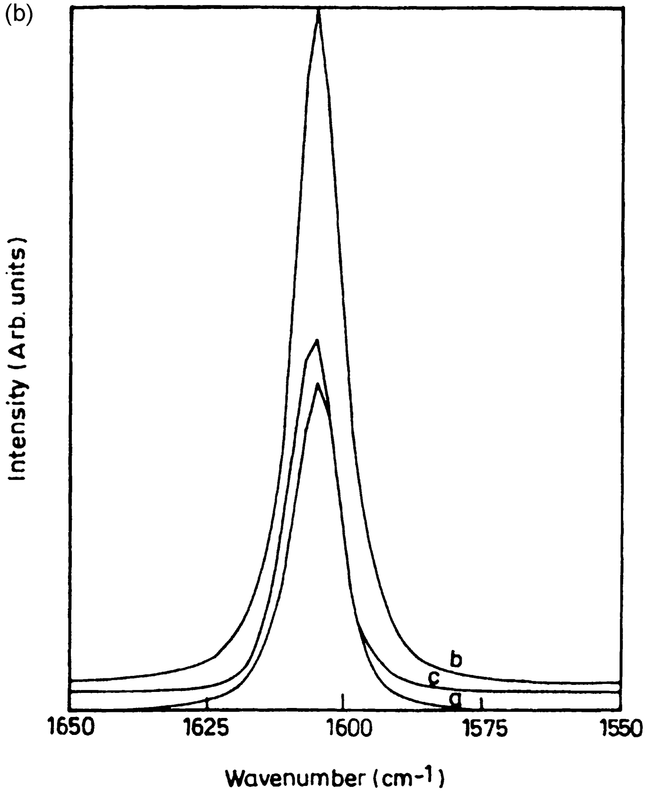

FIGURE 8(b) Continued.

half as intense as those of C_9 and C_{11}. Exactly the opposite behavior with respect to intensity of this band is observed in the Raman spectra of these compounds. The 1285 cm^{-1} peak is quite intense in both Raman and IR spectra. In the IR and Raman spectrum aromatic C–H in-plane deformation is observed at 1180 cm^{-1} (see Figures 4 and 5) [10].

In addition to the above, the strong bands appearing in the region of 780–850 cm^{-1} and 500–600 cm^{-1} in both IR and Raman spectra, in accordance with literature, are attributed to the CH out-of-plane deformations and the in-plane ring deformations of the ring, respectively [10,27,28,30]. From Figures 4 and 5 it can be clearly noted that the band profiles of C_9 and C_{11} are similar, whereas that of C_{10} is completely different in this region. The variation in the intensities of aromatic CC stretching and CN stretching is similar, indicating strong interaction of CN group with biphenyl part in C_{10} and strong polarizability of aromatic moiety.

CONCLUSIONS

The FTIR and FT-Raman spectra of C_9 and C_{11} show great similarity while differing with that of C_{10}. The differences are significant in the C–N stretching vibration and phenyl deformation regions. The peak positions of the C–N stretching vibration differs because of the difference in interaction between the CN dipole with that of phenyl ring, whereas the phenyl deformation bands show changes because of the difference in the dihedral angle between the phenyl rings in the biphenyl. From the IR and Raman CH stretching intensity ratios of C_9, C_{10}, and C_{11}, it can be readily concluded that the ordering of C_{10} differs from, that of C_9 and C_{11}. Also, the C_{10} system is more disordered compared to C_9 and C_{11}at room temperature. The molecular ordering in these compounds depends on the way the CN dipole interacts with the biphenyl moiety and the conformational ordering of the alkyl chain. The differences in the orientational ordering in the crystalline state of these compounds are clearly manifested in the vibrational spectra. The origin of disorder in these compounds lies in the packing differences in these crystals. In the high temperature smectic, nematic, and isotropic liquid phases, these packing differences, which manifest differently, form part of future investigations.

REFERENCES

[1] Gray, G. W. & Mosely, H.(1974). ***J. Chem. Soc. Perkin Trans.***, *1*, 97–102.
[2] Hudson, S. A. & Maitlis, P. M.(1993). ***Chem. Rev.***, ***93***, 861–885.
[3] Noirez, L., Keller, P., & Cotton, J. P. (1995). ***Liq. Crystals.***, ***18***, 129–148.
[4] Sheka, E. F. (1990). ***Sol. Phys. USP***, ***33***, 147–166.
[5] Rothschild, W. G., Perrot, M., & Jean-Marc, D. Z. (1991). ***J. Chem. Phys.***, ***95***, 2072–2079.
[6] Rotschild, W. G., Cavagnat, R. M., & Perrot M. (1987). ***J. Chem. Phys.***, ***118***, 33–43.
[7] Hatta, A., Nohara, H., & Suetaka, W. (1978). ***Bull. Chem. Soc. Jpn.***, ***51***, 967–973.
[8] Kaito, A. (1995). ***Mol. Cryst. Liq. Cryst.***, ***269***, 111–123.
[9] Perrot, M., De Zen, J. M., & Rothschild, W. G. (1992). ***J. Raman Spectrosc.***, ***23***, 633–636.
[10] Galbiati, E. & Zerli, G. (1986). ***J. Chem. Phys.***, ***84***, 3509–3518.
[11] Gray, G. W. & Winsor, P. A. (1974). ***Liquid Crystals and Plastic Crystals***, Vol. 1, (New York: Wiley).
[12] Gray, G. W. & Winsor, P. A. (1974). ***Liquid Crystals and Plastic Crystals***, Vol. 2, (New York: Wiley).
[13] Manisekaran, T., Bamezai, R. K., Sharma, N. K., & Prasad, J. S. (1997). ***J. Liq. Cryst.***, ***23***, 591–595.
[14] Manisekaran, T., Bamezai, R. K., Sharma, N. K., & Prasad, J. S. (1995). ***J. Mol. Cryst. Liq. Cryst.***, ***268***, 83–86.
[15] Manisekaran, T., Bamezai, R. K., Sharma, N. K., & Prasad, J. S. (1995). ***J. Mol. Cryst. Liq. Cryst.***, ***268***, 45–48.
[16] Maroncelli, M., Qi, S. P., Strauss, H. L., & Snyder, R. G. (1982). ***J. Am. Chem. Soc.***, ***104***, 6237–6247.
[17] Maroncelli, M., Strauss, H. I., & Snyder, R. G. (1985). ***J. Phys. Chem.***, ***89***, 5260–5267.

[18] Maroncelli, M., Strauss, H. I., & Snyder, R. G. (1985). ***J. Phys. Chem.***, ***89***, 4390–4395.
[19] Maroncelli, M., Strauss, H. I., & Snyder, R. G. (1985). ***J. Phys. Chem.***, ***82***, 2811–2824.
[20] Snyder, R. G. (1967). ***J. Chem. Phys.***, ***47***, 1315–1360.
[21] Snyder, R. G., Maroncelli, M., & Strauss, H. L. (1983). ***J. Am. Chem., Soc.***, ***105***, 133–134.
[22] Snyder, R. G. & Scherer, J. R., (1979). ***J. Chem., Phys.***, ***71***, 3221–3228.
[23] Snyder, R. G., Strauss, H. L., & Elliger, C. A. (1982). ***J. Phys. Chem.***, ***86***, 5145–5150.
[24] Snyder, R. G., Hsu, S. L., & Krimm S. (1977). ***Spectrochim. Acta.***, ***34A***, 395–405.
[25] Snyder, R. G., Srivatsavoy, V. J. P., Cates, D. A., Strauss, H. L., White, J. W., & Darset, D. L. (1994). ***J. Phys. Chem.***, ***98***, 674–684.
[26] Krim, Y., Strauss, H. L., & Snyder, R. G. (1989). ***J. Phys. Chem.***, ***93***, 485–490.
[27] Zerbi, G. & Sandroni, S. (1968). ***Spectrochim. Acta.***, ***24A***, 483–510.
[28] Zerbi, G. & Sandroni, S. (1968). ***Spectrochim. Acta.***, ***24A***, 511–528.
[29] Barrett, R. M. & Steele, D. (1972). ***J. Mol. Struct.***, ***11***, 105–125.
[30] Pulham, R. J. & Steele, D. (1984). ***J. Raman Spectrosc.***, ***15***, 217–223.
[31] Faiman, R. & Larsson, K. (1976). ***J. Raman Spectrosc.***, ***4***, 387–394.
[32] Proutiere, A., Legoff, D. & Chabanel, M. (1988). ***J. Raman Spectrosc.***, ***178***, 49–61.
[33] Casal, H. L. & McElhaney, R. N. (1990). ***Biochemistry***, ***29***, 5423–5427.
[34] Ziegler, W. & Blume, A. (1995). ***Spectrochimica Acta***, ***51A***, 1763–1778.